DEPENDENCY OF THE INITIAL STAGE OF STRESS CORROSION CRACKING BEHAVIOR OF AUSTENITIC STAINLESS STEEL ON THE STRESS LEVEL

T. Yagasaki*, Y. Kimura* and T. Kunio**

**Department of Chemical Engineering, Kogakuin University, Tokyo, Japan*
***Faculty of Science and Engineering, Keio University, Yokohama, Japan*

ABSTRACT

In this paper, the initial stage of stress corrosion cracking behavior of austenitic stainless steel SUS304 was investigated in boiling 42% magnesium chloride aqueous solution. Nucleation and initial propagation of stress corrosion micro cracks were analyzed both in surface and in fracture surface from microstructural aspect in a wide range of stress from around threshold stress where no plastic deformation occurred macroscopically to 0.2% proof stress. The main results are summarized as follows;

(1) Stress corrosion cracking behavior at the initial stage is dependent upon the stress level. Namely, at higher stress levels, intercrystalline cracking originating from triple grain boundaries occurred, but as the stress level was lowered, it was replaced with transgranular one accompanied with corrosion grooves.

(2) Micro crack growth from the small corrosion grooves is an important factor determining the value of the threshold stress of material used.

(3) At a stress level near 0.2% proof stress, the stress corrosion crack nucleats from broken point of the passive film on triple grain boundaries where the material is concentrically strained and it propagates to interconnect triple grain boundaries.

KEYWORDS

Stress corrosion cracking; initial stage behavior; stress level dependency; triple grain boundaries; corrosion groove.

INTRODUCTION

There are many published papers (e.g. Denhard, 1961) on stress corrosion cracking (SCC) of austenitic stainless steels in chloride aqueous solution. Attaching too much importance to acceleration of cracking, however, many of these studies were conducted at stress levels high enough to cause plastic deformation. Thus, few (Kumada, 1973; Silcock, 1979, 1982) were concerned in the nucleation mechanism and propagation characteristics of stress corrosion cracking at lower stress levels that are more important in considering the

resistance of austenitic stainless steels used for structural materials in corrosive environment. Furthermore, to elucidate the mechanism of fracture, it is necessary to have a good understanding of the process of fracture itself. The fracture morphology related to such process (Koterazawa and Shimo, 1978) has not been studied systematically. Moreover, in the previous studies concerning the fracture morphology, the very early stage of stress corrosion cracking that is substantially important has not been fully discussed with many aspects left to be studied in future.

In the present study, SCC tests were made with a wide range of stress from around threshold stress where no plastic deformation occurred macroscopically to 0.2% proof stress. In these tests, the characteristics of stress corrosion micro cracks at their initial stages were examined both in surface and in fracture surface from microstructural point of view. As a result, the stress level dependency of stress corrosion crack behavior is recongnized. The fracture mechanism at higher stress levels is also discussed.

TEST MATERIALS AND EXPERIMENTAL PROCEDURES

In this study, rods (ϕ18mm) of the commercial austenitic stainless steel SUS304 were used for test materials. Table 1 shows the chemical composition of this steel. Twe materials that differed in grain size were used: (a) as received material itself that had already undergone a solid solution treatment at 1353K followed by water cooling before supply, ASTM Grain Size No. 7.5, mean grain size 45μm, 0.2% proof stress 244MPa; and (b) laboratory treated material that underwent an hour solid solution treatment at 1423K followed by water cooling to as received material in our laboratory, ASTM Grain Size No. 5.1, mean grain size 69μm, 0.2% proof stress 230MPa. For usual stress corrosion cracking test at a wide stress range from around threshold stress to 0.2% proof stress, both specimens were used, while the nucleation and initial propagation of stress corrosion cracking were mainly investigated using the latter specimen.

These materials were shaped into the geometry shown in Figure 1. The parallel test area of these specimens was finished by acetateperchlorate electropolishing. Immediately before testing, specimens were immersed in methyl alcohol for full degreasing. They were tested under fully immersed condition in a corrodant bath (Pyroceram vessel) equipped with a reflux condenser using a constant load type uniaxial tension tester. The maximum tensile load of this tester was 3ton.

The corrodant bath was composed of 42% magnesium chloride aqueous solution prepared in conformity to JIS G 0576 by dissolving extra pure magnesium chloride ($MgCl_2 \cdot 6H_2O$) as specified in JIS K 8159 in deionized water having a specific resistance over 50kΩm. The total volume of bath was 0.5dm³. All tests were conducted at the boiling point of the corrodant, which was always maintained at 416±0.5K.

In order to examine stress corrosion cracking at its initial stage, the specimen was unloaded and detailed observation was conducted when cracks grew to about 200μm long covering about a few grains. Furthermore, to examine particularly the cracking characteristic on fracture surface, these specimens were fractured by hydraulic fatigue testing machine in air. Moreover, the constant potential etching method (Ohtani and Iba, 1969; Ohtani, Aihara and Takamoto, 1969) by a potentiostat was applied in an electroetchant (1N H_2SO_4+100mg/L NH_4SCN), in case when it is necessary to produce oriented etch pits on fracture surfaces to see whether the fracture was intercrystalline or not.

To examine the microstructural characteristics of stress corrosion cracking, both an ordinary optical microscope and a scanning electron microscope (Hitachi Model S-450) were used for observation.

RESULTS AND DISCUSSIONS

Results of Stress Corrosion Cracking Tests

The σ-t curves of Figure 2 show the results of 50hours stress corrosion cracking tests. Estimates of the threshold stress from these curves gave for the two kinds of test specimens, that is the as received material and the laboratory treated material, under the given test environment were around 130 and 110MPa, respectively. Test results given in the following two sections refer mainly to the laboratory treated material tested in the stress range from the threshold stress to the 0.2% proof stress.

Dependency of the Initial Stress Corrosion Cracking on the Stress Level

Many investigators (e.g. Smith, 1969) tried to explain the nucleation and propagation of stress corrosion cracking at higher stress levels from electrochemical point of view, ascribing the nucleation or generation of stress corrosion cracks to the preferential anodic dissolution in newly exposed surface areas where the passive film was broken as a result of formation of slip steps under an applied stress. The present authors also studied the stress corrosion cracking at the stress level of 235MPa, which is close to the 0.2% proof stress. After 4minutes (around 5% of the estimated time to failure), authors observed nucleation and propagation of cracking as shown in Figure 3. At this level, though there were observed slip bands in the whole surface of specimen, no nucleation of stress corrosion cracking was detected in corrosion grooves along slip lines. It was found that the originated crack propagated along grain boundaries to interconnect triple points as shown in Figure 4. In this case, the ratio of crack propagation path through grain boundary is estimated about 98%. In this figure, the grain boundaries from which the cracks originated are shown by arrows.

In the past, there were papers asserting that in the highly concentrated boiling magnesium chloride aqueous solution the stress corrosion cracking directly occurred and propagated without any pitting. In recent years, however, it was reported (Kumada, 1973) that at lower stress levels the nucleation and propagation of stress corrosion cracking were preceded by the formation of micro-corrosion pits. Also in the present study, this was recognized at stress levels not higher than 180MPa. Figure 5 shows an example of such stress corrosion cracking behavior, which was observed at a stress level of 180MPa after 20minutes (around 20% of the estimated time to failure). The stress corrosion cracks generated still primarily at triple grain boundaries as shown in Figure 5(a). In a smaller number of cases, however, these cracks were nucleated at micro corrosion pits and propagated to interconnect these pits as shown in Figure 5(b).

As the stress level was lowered, the number of slip lines in the surface decreased and stress corrosion cracks sometimes propagated along transgranular paths. The photograph of Figure 6(a) refers to the initial stress corrosion crack observed in the surface at a stress level of 150MPa after 52minutes (around 37% of estimated time to failure), while Figure 6(b)(c) are matching photographs for fracture surface of this crack. As shown in Figure 6(a), cracks at this stress level were often locally accompanied with corrosion groove where few slip lines were observed. They propagated straightly in a

direction that was perpendicular to the principal axis of stress. At this stress level, the same type of nucleation and propagation of crack were observed also in case when no slip line could be detected. Many cracks formed at grain boundaries in surface where slip lines gathered propagated to a certain depth along such boundaries to form intercrystalline fracture surface. The ratio of crack path through grain boundaries would be estimated to be about 70% in the surface, while in the fracture surface it would become about 25%. From these facts, it could be concluded that there is a transition region around a stress level of 150MPa where the major factor causing the nucleation and propagation of initial stress corrosion crack in surface changes from slip deformation to corrosion groove formation.

At still lower stress levels, many stress corrosion cracks that originated from corrosion grooves were observed. Figure 7 refers to such a surface morphology showing the propagation of stress corrosion cracks at 132MPa after 120minutes (around 60% of the estimated time to failure). At this stress level, few slip lines were detected and the cracks started from the bottom of corrosion grooves. They propagated transgranularly to interconnect several corrosion grooves, partly becoming fine cracks without any grooves. The ratio of crack paths through grain boundaries could be estimated to be about 13% in surface. This stress level was in a region where cracks originating from corrosion grooves were dominant. Figure 8 is a matching photograph of fracture surface of stress corrosion cracking at its initial stage that was produced at the same stress level. Through examing the morphology of facet pits on fracture surface, the percentage of grain boundaries in the fracture surface was estimated around 13%, which was almost equivalent to the corresponding estimation in surface.

The ratio of intergranular cracking which was evaluted at various stress levels are summarized in Figure 9. In this figure, the broken line represents the intergranular ratio of stress corrosion cracking in surface at its initial stage, while the solid line shows that in fracture surface. This figure evidently indicates that the characteristics of stress corrosion cracking at its initial stage depend on the stress level. Intercrystalline cracking originates from triple grain boundaries at higher stress levels, but it was replaced with transgranular cracking accompanied with corrosion groove as the stress level was lowered. Also in this figure, there is the difference in the intergranular ratios between surface and fracture surface at the intermidiate stress levels examined. This difference was remarkable in the transition stress region where the major factor causing stress corrosion cracking changed from the slip deformation to the corrosion groove formation. As one of the reasons for this difference, it would be pointed out that the surface of specimen was liable to cause easy plastic deformation because of its being free from mechanical restrictions.

Nucleation and Propagation of Cracks from Triple Grain Boundaries at Stress Levels around 0.2% Proof Stress

In the previous section, the dependency of the initial stress corrosion cracking behavior on the stress level was shown. In this section, some discussion will be made particularly about such cracking behavior at higher stress levels. Figure 10(a) and (b) show morphologies of initial stress corrosion crack observed in the surface of a test piece at the stress level of 235MPa which is around the 0.2% proof stress, while Figure 10(c) and (d) are matching photographs of fracture surface. These figures indicate that at this stress level the stress corrosion crack nucleates at triple grain boundaries (Pickering and Swann, 1963) and propagate along grain boundaries to interconnect triple grain boundaries. Therefore, it was recognized that the fracture

surface formed by stress corrosion cracking was the grain boundary itself. This was also indicated from the morphologies of the facet pits created electrochemically on both sides of the fractaure surfaces. Furthermore, fracture surface were generally rather rounded under the effect of corrosive environment and there were detected some traces of electrochemical dissolution at triple grain boundaries as shown in photographs 10(e) and (f). It is concluded from these observations that around 0.2% proof stress the stress corrosion crack starts from broken points of the passive film on triple grain boundaries where the material is concentrically strained and it propagates to interconnect triple grain boundaries.

CONCLUSIONS

Stress corrosion cracking behavior at the initial stage of austenitic stainless steel SUS304 was investigated in boiling 42% magnesium chloride aqueous solution. Nucleation and initial propagation of stress corrosion micro cracks were analyzed both in surface and in fractaure surface from microstructural aspect in a wide stress range from around threshold stress to 0.2% proof stress. The main results are summarized as follows;

(1) Stress corrosion cracking behavior at the initial stage is dependent upon the stress level. Namely, at higher stress levels, intercrystalline cracking originating from triple grain boundaries occurred, but as the stress level was lowered, it was replaced with transgranular one accompanied with corrosion grooves.

(2) Micro crack growth from the small corrosion grooves was an important factaor determining the value of the threshold stress of material used.

(3) At a stress level near 0.2% proof stress, the stress corrosion crack nucleates from broken point of the passive film on triple grain boundries where the material is concentrically strained and it propagates to interconnect triple grain boundaries.

REFERENCES

Denhard, E.E. Jr. (1960). Effect of composition and heat treatment on the stress corrosion cracking of austenitic stainless steels. Corrosion, 16, 359t-369t.

Koterazawa, R., and D. Shimo (1978). Stress corrosion cracking of a SUS304 stainless steel in $MgCl_2$ solution. J. Japan Institute of Metals, 27, 1158-1164.

Kumada, M. (1973). Effects of alloy composition on the stress corrosion cracking susceptibility of stainless steels in high temperature chloride solution. J. Japan Soc. Corrosion Engineering, 22, 274-285.

Ohtani, N., K. Aihara, and S. Takamoto (1969). Observation on etch pits on a 18-8 stainless steel by motion pictures. J. Japan Institute of Metals, 33, 432-436.

Ohtani, N., and T. Iba (1969). On the relation between stress corrosion cracking and crystallographic orientation in 18-8 stainless steel. J. Japan Institute of Metals, 33, 781-785.

Pickering, H.W., and P.R. Swann (1963). Electron metallography of chemical attack upon some alloys susceptible to stress corrosion cracking. Corrosion, 19, 373t-389t.

Silcock, J.M. (1973). Effect of acidity and applied potential on the stress corrosion cracking of type 316 austenitic steel in $MgCl_2$. Br. Corros. J., 14, 206-215.

Silcock, J.M. (1982). Nucleation and growth of stress corrosion cracks in austenitic steels with varying Ni and Mo contents. Corrosion, 38, 144-156.

Smith, T.J., and R.W. Staehle (1969). Role of slip step emergence in the early stages of stress corrosion cracking in face centered iron-nickel-chromium alloys. Corrosion, 23, 117-129.

TABLE 1 Chemical Composition (wt%)

C	Si	Mn	P	S	Ni	Cr
0.05	0.28	0.39	0.034	0.025	8.25	18.25

(SUS 304)

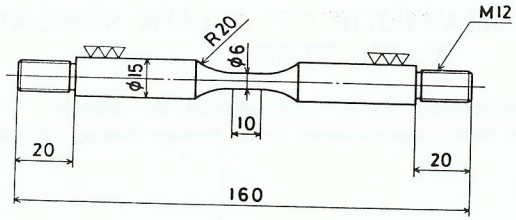

Fig. 1. Dimensions of Specimen Used. (mm)

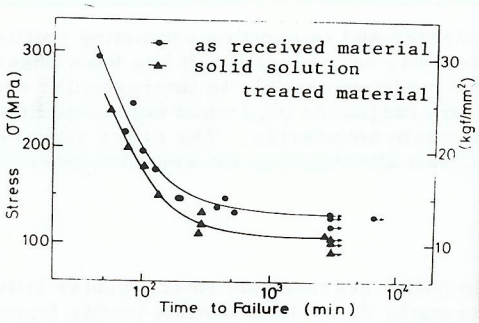

Fig. 2. Results of SCC Tests.

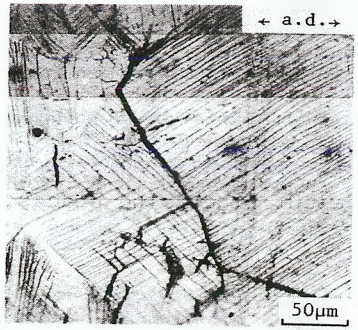

Fig. 3. Stress Corrosion Cracking Behavior at Level of 0.2% Proof Stress.

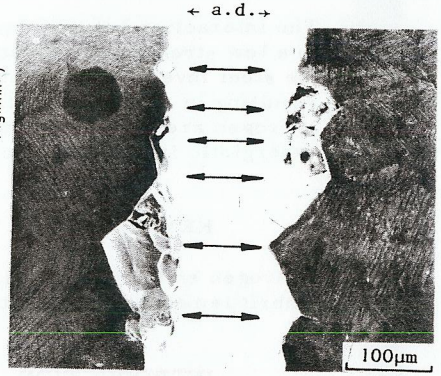

Fig. 4. Crack Propagated along Boundaries to Interconnect Triple Points of Grain Boundaries.

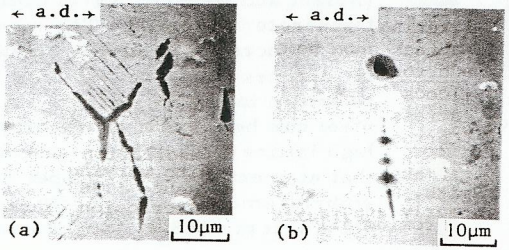

Fig. 5. Nucleation and Propagation of Stress Corrosion Cracks at Stress Level of 180MPa.
(a) Cracks Nucleated at Triple Grain Boundaries.
(b) Cracks Nucleated at Micro Pits.

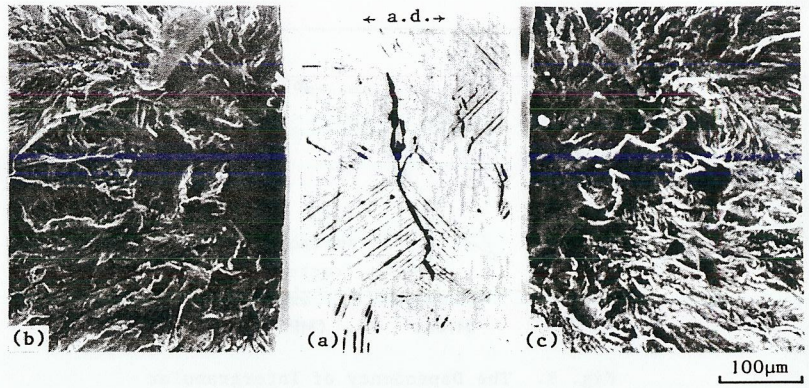

Fig. 6. Stress Corrosion Cracking Behavior at Stress Level of 150MPa.
(a) Surface Morphology.
(b)(c) Matching Photographs of Fracture Surface.

Fig. 7. Stress Corrosion Cracks Observed in Surface. σ=132MPa

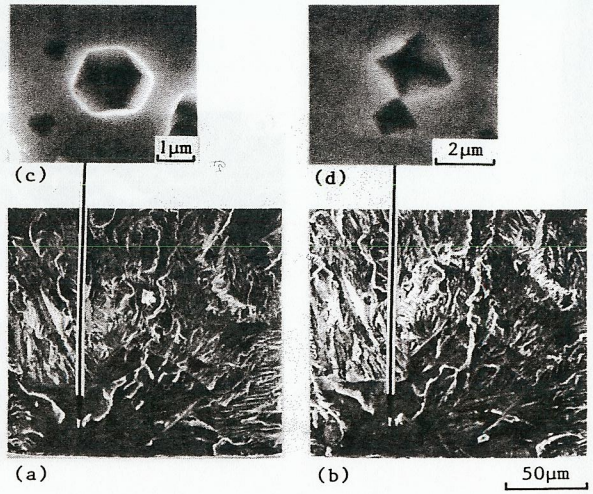

Fig. 8. Fracture Surface of SCC at a Stress Level of 132MPa.
(a)(b) Matching Photographs.
(c)(d) Facet Pits.

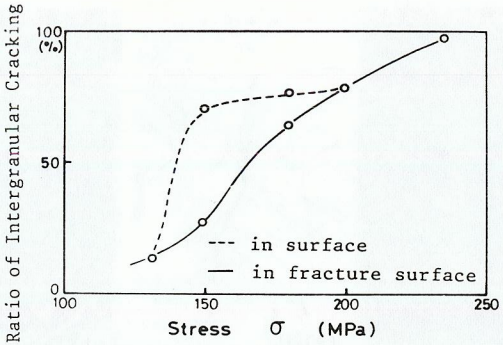

Fig. 9. The Dependency of Intergranular Cracking Ratio on Stress Levels.

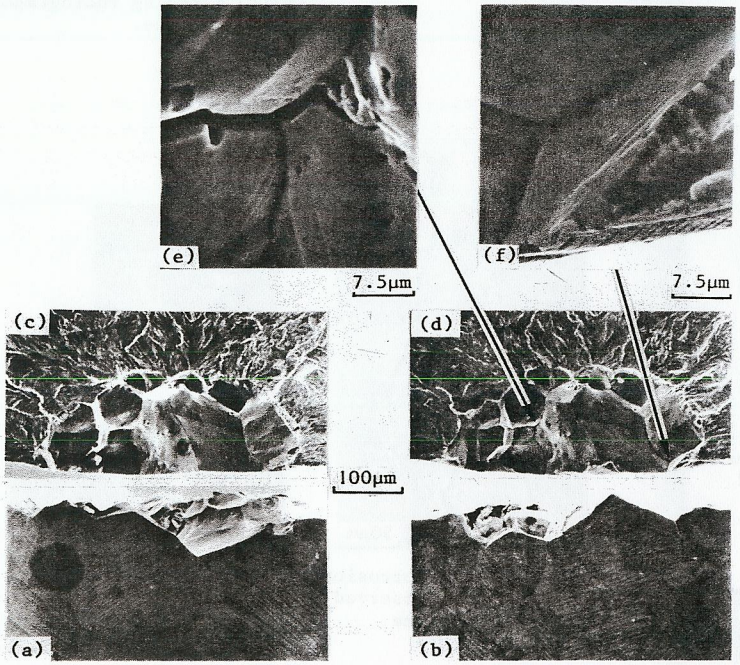

Fig. 10. Morphologies of Initial Stress Corrosion Crack Observed at the Stress Level of 235MPa.
(a)(b) Surface. (c)(d) Fracture Surface.
(e)(f) Some Traces of Electorochemical Dissolution on Fracture Surface.